ChemComm

COMMUNICATION

View Article Online
View Journal | View Issue

Cite this: *Chem. Commun.*, 2025, **61**, 18673

Received 13th February 2025,
Accepted 17th October 2025

DOI: 10.1039/d5cc00783f

rsc.li/chemcomm

Base-mediated alkynyl-cubane to Cu_8-alkynide cluster transformation

Arvind Kumar Gupta,[a] Océane Y. O. Fayet,[ab] Lei Tian,[a] Raphael J. F. Berger,[c] Reiner Lomoth[a] and Andreas Orthaber*[a]

We demonstrate that a copper cubane cluster $[Cu_4Cl_4(LH)_4]$ can be converted into an octanuclear cluster $[Cu_8L_8]$ through deprotonation of the triisopropylacetylene ligands. The former displays exclusively side-on coordination of the terminal acetylene, while the latter exhibits both side-on and end-on coordination of the deprotonated acetylide moiety. The octanuclear complex shows solid-state emission around 640 nm, while the cubane displays a thermochromic emission shifting from 563 nm at r.t. to 608 nm upon cooling to 77 K.

Copper alkynyl complexes have attracted great attention due to their structural diversity, and fascinating photophysical properties. Cuprophilic interactions often result in beneficial optical properties and provide novel opportunities in the development of optoelectronic materials.[1,2] Recent advances concerning the synthesis and characterization of well-defined copper(I) alkynyl complexes have led to new applications in supramolecular chemistry and as materials with interesting emissive properties.[3–6] The isolation and structural elucidation of various organo-copper(I) compounds has led to the development of novel strategies towards interesting organic frameworks.[7,8] Apart from this, organo-copper(I) complexes are frequently encountered as key intermediates in copper(I)-mediated or copper-catalysed organic transformations.[9] Most importantly copper(I) alkynide species are crucial intermediates in different C–C cross coupling reactions, *e.g.* Sonogashira, Glaser Hay Chadiot-Chodkiewicz and the Huisgen Copper-catalysed azide–alkyne cycloaddition reactions.[10,11]

Copper(I) cubane motifs display a large variety of ligand/counter ion combinations. Halide containing cubanes $[Cu_4X_4L_4]$ (where X = Cl, Br, I) are reported for a large variety of ligands.[12–15]

These systems also show fascinating optical properties, such as thermally activated delayed fluorescence and other fascinating excited state dynamics and responsive behavior.[13,16,17] Notably, the Cu-cubane is typically highly stable and allows for post-synthetic modifications.[18,19] Another group of cubanes are the Cu-acetylide family (where X = $^-C\equiv CR$), where the four copper(I) atoms form a distorted tetrahedral shape and each triangular shaped Cu_3-unit is capped with the terminal alkynide.[20–22] However, only very few solid-state structures have been reported to have an alkyne (RC ≡ C–H) ligand directly coordinating to copper(I) motifs.[23–25] Mononuclear Cu-alkynyl derivatives are only stable with additional ligands or binding sites within the alkynyl ligand (Fig. 1).[26–28] In this communication, we report the missing puzzle piece in these Cu-cubane structures. The well-established $[Cu_4Cl_4]$-core is stabilized by alkynyls acting as neutral donor ligands. This cluster (**1**) $[Cu_4\{\mu_1\text{-}\eta^2\text{-}HC\equiv CSi(^iPr)_3\}_4(\mu_3\text{-}Cl)_4]$, in which four triisopropylsilyl acetylene ligands (**L**–H) stabilize a $[Cu_4Cl_4]$-core, can be transformed into an acetylide cluster by addition of triethylamine in a dehydrohalogenation reaction giving rise to an octanuclear copper(I) complex, $[Cu(C\equiv C\text{-}Si^iPr_3)]_8$ (**2**). The solid

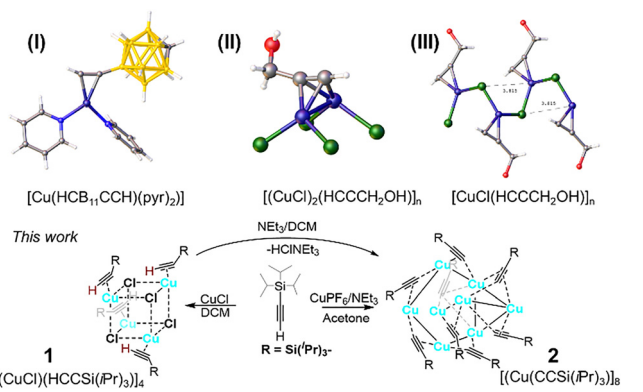

Fig. 1 Basic structural motif of selected Cu(I)-alkynyl coordination compounds (**I–III**). Synthetic approach to the alkynyl copper cubane **1** and octanuclear copper alkynide cluster **2**.

[a] *Department of Chemistry, Ångström Laboratories, Uppsala University, Box 523, 751 20 Uppsala, Sweden. E-mail: andreas.orthaber@kemi.uu.se*
[b] *ENSICAEN National Graduate School of Engineering and Research Center, Caen, France*
[c] *Department Chemistry and Physics of Materials, Paris Lodron Universität Salzburg, Jakob-Haringerstr. 2A, 5020 Salzburg, Austria*

state and optical properties of both complexes are studied in detail, and further supported by means of theoretical calculations.

Formation of cubane **1** $[Cu_4(HC{\equiv}CSi(({}^{i}Pr)_3)_4Cl)_4]$ can be achieved by the reaction of triisopropylsilyl acetylene and CuCl in dry DCM in the absence of any base. Expectedly, no deprotonation of the acetylenic hydrogens occurred during the complexation as evidenced by IR analysis of the solid material, which was obtained after removal of all volatiles. The identity of this material was further corroborated by single crystal X-ray diffraction studies (SC-XRD, *vide infra*). Further attempts to characterize **1** in solution (NMR and ESI-MS) failed, suggesting deaggregation of the cubane motif. However, addition of triethylamine to this solution (DCM) immediately results in a colour change from light yellow to deep orange indicating deprotonation of the acetylenic hydrogens and ultimately formation of **2**, $[Cu(C{\equiv}C{}^{i}Pr_3Si)]_8$, as evidenced by spectroscopic and crystallographic analysis. Alternatively, complex **2** can be obtained by the reaction of **L**–H and $[Cu(CH_3CN)_4PF_6]$ in the presence of triethylamine.

IR analysis of complex **1** shows that the typical C≡C stretching vibration of the ligand is shifted by 150 cm^{-1} to lower wavenumbers (1881 cm^{-1}, *cf.* **L**–H 2032 cm^{-1}) indicative of strong interaction of the triple bond with the metal core, through electron donation from the metal to antibonding orbitals of the ligand. Additionally, we see a band at 3197 cm^{-1} and multiple bands between 550 and 700 cm^{-1} attributable to the terminal C–H stretching (**L**–H: 3294 cm^{-1}) and the bending modes (**L**–H: 675 cm^{-1}), illustrating the coordination effects on the terminal acetylene C–H moiety. For complex **2** a shifted C≡C stretching vibration of 1944 cm^{-1} is consistent with a terminal coordination of the acetylide carbon.[23] In order to interpret the IR spectra of **1** and **2** unambiguously, we have calculated their respective IR frequencies using DFT (TPSS/def2-TZVPP with a scaling factor of 0.943) supporting these assignments (see Fig. S3 and S4). The DFT calculation of **1** predicts a C≡C stretching frequency of 1897 cm^{-1} closely matching with the observed band at 1880 cm^{-1}. Also, the calculated alkynyl CH stretching frequency of 3225 cm^{-1} (exp. 3197 cm^{-1}) in **1** is slightly hypsochromically shifted compared to the free ligand 3277 cm^{-1} (exp. 3420 cm^{-1}). For cluster **2**, multiple bands for the C≡C stretching modes are calculated (1980, 1950, and 1897 cm^{-1}); however, experimentally only one distinguishable feature at 1940 cm^{-1} (besides two minor side-bands) was observed, matching the expected range. Complex **2** is persistent in solution and ESI-MS of **2** gives a prominent peak of **2** ionized with one additional copper atom $[Cu_8(C{\equiv}C{}^{i}Pr_3Si)_8] + Cu^+$ at m/z = 2022.49156. Proton and carbon NMR data suggest that the structure is dynamic in solution showing only one set of triisopropylsilylacetylide signals. The acetylide signals are detected at 94.8 and 58.9 ppm in the $^{13}C\{^1H\}$-NMR spectra, *i.e.* strongly shielded resonances compared to the free acetylene, as previously observed for silver acetylide systems (see Fig. S2, SI).[29]

The solid-state structures of **1** and **2** were determined by single crystal X-ray diffraction. The solid-state structure of **1** is solved in the triclinic space group $P\bar{1}$ with one full molecule in the asymmetric unit. From the crystal structure analysis, it is evident that the $[Cu_4Cl_4]$ core in **1** adopts a highly distorted cubane arrangement

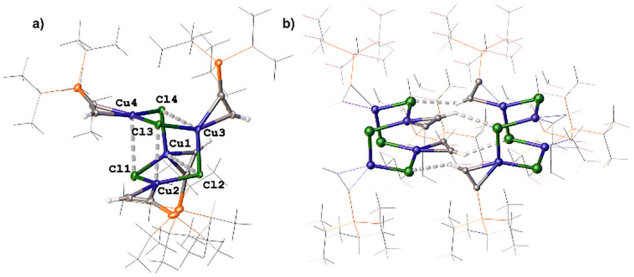

Fig. 2 Solid-state structure of (**1**). (a) The Cu_4Cl_4-core and SiCCH drawn as thermal ellipsoids (50% probability levels); ^{i}Pr-groups are rendered as wire frame for clarity. (b) Weak hydrogen bonding (CC–H···Cl) linking clusters of **1** into a 1D-network.

(Fig. 2a). We speculate that this distortion might be linked to the hydrogen bond of the actylenic proton with a neighbouring cluster chloride atom (Fig. 2b). Each of the four copper atoms is tetrahedrally coordinated by three bridging chloride ions (μ_3-Cl) and the acetylene ligand. The latter coordinates symmetrically side-on (μ_1-η^2) with Cu–$C_{(C\equiv C)}$ distances in the range of 1.976(7)–2.040(1) Å. The Cu–Cl bond lengths vary significantly ranging from 2.255(4) to 3.272(13) Å. The Cu···Cu distances range from 3.383(11) to 3.681(5) Å indicating only weak cuprophilic interactions as these distances are significantly longer than the sum of van der Waals radii for copper (2.8 Å). This type of cubane structure is comparable to those typically observed for phosphine and nitrogen donor ligands.[12,30–32] To the best of our knowledge this is the first observation of a cubane-like structure supported by a neutral acetylene ligand. The acetylene clearly has triple bond character with bond distances ranging from 1.220(10) to 1.241(10) Å while displaying significant distortion from linearity (Si–C≡C angles ranging from 156.7(6) to 158.2(6)°).[33] However, the triple bond length is markedly elongated compared to unsupported silyl acetylenes (*ca.* 1.181 to 1.197 Å).[34] Such alkyne coordination to Cu(I) centres is rather rare (*ca.* 30 reports in CSD) and spans a variety of mono- to polynuclear complexes (0D to 2D-coordination compounds).[23,24,26,35] A more pronounced elongation of coordinated alkynyls is seen in mononuclear W (*ca.* 1.27 Å)[35,36] and Nb (1.28 Å)[37] complexes. The large distortion from linearity and elongation in **1** qualitatively supports the observed shift of the C≡C stretching frequency ($\Delta\nu_s$ = −151 cm^{-1}), which is also reproduced in our *ab initio* calculations (*vide infra*), and in line with acetylene adducts of copper(I) and silver(I).[38] Notably, the sterically demanding TIPS groups shield the individual clusters and allow only for very weak hydrogen bonding of the alkynyl-H to a chloride corner of a neighbouring cluster (Fig. 2b). The ^{i}Pr-groups offer a large degree of rotational freedom evidenced by the disorder and large ADPs.

Suitable crystals of **2** for single crystal X-ray measurement were obtained by the slow evaporation of a solution of **2** in acetone and a few drops of ethanol. The crystal structure of **2** is solved in the orthorhombic space group $P2_12_12_1$. The structure consists of a charge neutral eight copper atom framework coordinated with an equal number of triisopropylsilylacetylide ligands. Four different coordination modes are identified: five μ_2-$\eta^1\eta^2$, and one each of μ_3-$\eta^1\eta^1\eta^1$, μ_3-$\eta^1\eta^1\eta^2$, and μ_3-$\eta^1\eta^2\eta^2$.

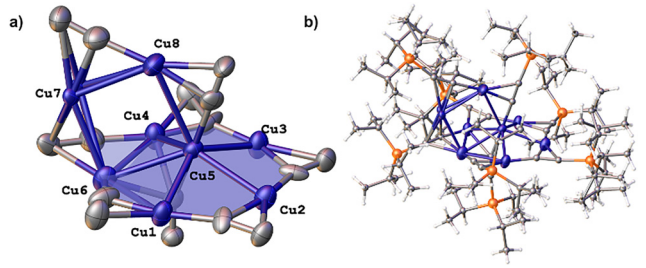

Fig. 3 Solid-state structure plots of **2**. (a) Cu-core and alkynide C-atoms (ADPs at 50% probability level) highlighting the basal plane consisting of $\{Cu_5(CC)_5\}$. The Cu7/Cu7A shows a positional disorder (0.1/0.9). (b) View including the TIPS groups (stick model) illustrating the steric shielding. All disordered TIPS groups are shown.

The core of the cluster forms a unique "kite" arrangement (Fig. 3a) and can be described by a copper-acetylide pentagon (Cu1-4, 6) holding one additional Cu atom (Cu5) *ca.* 0.81 Å above the center of that plane combined with two Cu-centres (Cu7/Cu7A[39] and Cu8). The Cu···Cu distances from the central Cu5 to the five membered ring Cu-atoms are on average shorter (*ca.* 2.65 to 278 Å), whereas "added" Cu7/Cu8 have longer Cu–Cu distances (Cu5–Cu8 2.951(3), Cu6–Cu7 2.814(3), Cu6–Cu7A 2.692(2)). This added copper dimer is held above one face assisted by three bridging acetylide ligands.

This complex motif reflects the diversity of Cu(I) alkynide coordination modes and the tremendous effect of the steric demand of the alkynide ligands as seen in many other examples.[3,40–42] Fig. 4 summarizes the different coordination modes observed for cluster **1** and **2**, respectively. While (**1**) shows exclusive side-on coordination (η^2), the acetylide complex (**2**) shows a variety of bridging coordination modes. The electronic absorption spectra of solid cluster **1** and **2** display a common UV absorption band at about 370 nm and a lower energy absorption around 420 nm characteristic of **2** (Fig. S9 and S10). Both clusters show solid state photoluminescence (Fig. 5) with orange emission for **2** (λ_{em} = 640 nm at r.t. and 77 K) and a temperature dependent emission maximum for **1** (λ_{em} = 563 nm at r.t., 608 at 77 K). The excitation spectra (Fig. S11) are tracing the 370 nm absorption band of both clusters while the visible absorption of **2** matches the excitation spectrum only at low temperature. (Emission lifetime measurements revealed for both complexes a multiphasic decay with the dominating components in the sub-ns regime; Fig. S7 and S8). In depth theoretical studies (of extended solid-state models) and structural investigations will be needed to elucidate the electronic and geometric factors

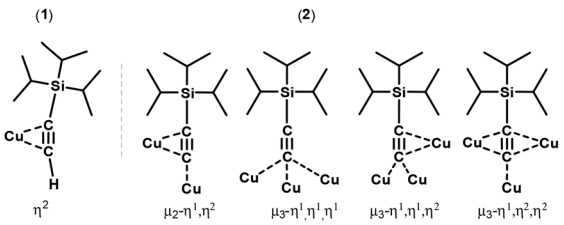

Fig. 4 Observed coordination modes in complex **1** (left) and **2** (right).

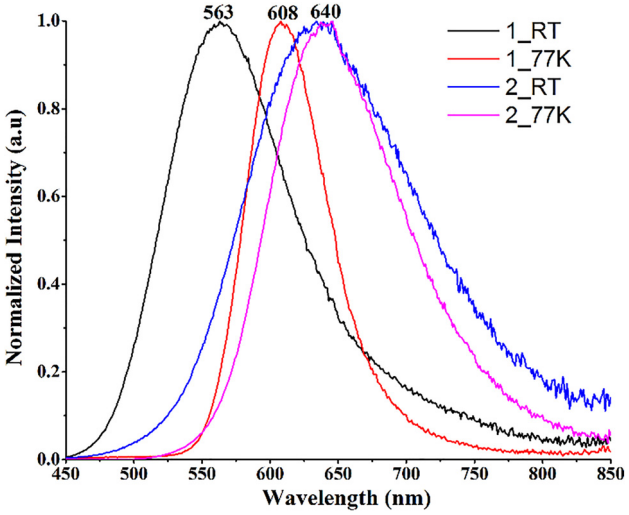

Fig. 5 Emission spectra in the solid state of **1** and **2** at 298 and 77 K (at $\lambda_{exc.}$ = 365 nm).

governing these emission profiles. At the moment detailed explanations of the marked different photophysical behaviour of these complexes remain elusive.

In summary we have presented a cubane motif consisting of a $[CuCl]_4$ core surrounded by neutral triisopropylsilyl acetylene ligands, which can be transformed into an octanuclear Cu-acetylide cluster upon deprotonation with an organic base. As such, these motifs are relevant structures in various organic transformations including C–C coupling and Click reactions. Moreover, interesting luminescent behaviour was investigated revealing a thermochromic behaviour of the cubane **1**, in contrast to the unchanged emission of the acetylide cluster **2**. This facile conversion and the variable opto-electronic properties promise interesting applications of these materials as sensors, or in organic electronics.

Conflicts of interest

There are no conflicts to declare.

Data availability

The data supporting this article have been included as part of the supplementary information (SI). Supplementary information: synthesis details and spectroscopic data of the complexes. Details of quantum chemical calculations. See **https://doi.org/10.1039/d5cc00783f**.

CCDC 2239140 (**1**) and 2239141 (**2**) contain the supplementary crystallographic data for this paper.[43a,b]

References

1 R. Nast, *Coord. Chem. Rev.*, 1982, **47**, 89–124.
2 V. W.-W. Yam and K. K.-W. Lo, *Chem. Soc. Rev.*, 1999, **28**, 323–334.
3 X.-Y. Chang, K.-H. Low, J.-Y. Wang, J.-S. Huang and C.-M. Che, *Angew. Chem., Int. Ed.*, 2016, **55**, 10312–10316.

4 H. Lang, A. Jakob and B. Milde, *Organometallics*, 2012, **31**, 7661–7693.
5 S. N. Panda, P. Pradhan, S. Nath, J. Mohapatra, B. K. Patra and B. P. Biswal, *Chem. Commun.*, 2025, **61**, 2536–2539.
6 V. W.-W. Yam, *J. Organomet. Chem.*, 2004, **689**, 1393–1401.
7 M. Ito, D. Hashizume, T. Fukunaga, T. Matsuo and K. Tamao, *J. Am. Chem. Soc.*, 2009, **131**, 18024–18025.
8 W. Geng, J. Wei, W.-X. Zhang and Z. Xi, *J. Am. Chem. Soc.*, 2014, **136**, 610–613.
9 T. Tsuda, T. Hashimoto and T. Saegusa, *J. Am. Chem. Soc.*, 1972, **94**, 658–659.
10 A. M. Thomas, A. Sujatha and G. Anilkumar, *RSC Adv.*, 2014, **4**, 21688–21698.
11 A. Makarem, R. Berg, F. Rominger and B. F. Straub, *Angew. Chem., Int. Ed.*, 2015, **54**, 7431–7435.
12 T. Agou, N. Wada, K. Fujisawa, T. Hosoya, Y. Mizuhata, N. Tokitoh, H. Fukumoto and T. Kubota, *Inorg. Chem.*, 2018, **57**, 9105–9114.
13 Y. V. Demyanov, Z. Ma, Z. Jia, M. I. Rakhmanova, G. M. Carignan, I. Y. Bagryanskaya, V. S. Sulyaeva, A. A. Globa, V. K. Brel, L. Meng, H. Meng, Q. Lin, J. Li and A. V. Artemev, *Adv. Opt. Mat.*, 2024, **12**, 2302904.
14 M. Białoń, B. Dziuk and V. Olijnyk, *Eur. J. Inorg. Chem.*, 2020, 1790–1793.
15 E.-M. Rummel, M. Eckhardt, M. Bodensteiner, E. V. Peresypkina, W. Kremer, C. Gröger and M. Scheer, *Eur. J. Inorg. Chem.*, 2014, 1625–1637.
16 A. Kobayashi, Y. Yoshida, M. Yoshida and M. Kato, *Chem. – Eur. J.*, 2018, **24**, 14750–14759.
17 R. Utrera-Melero, B. Huitorel, M. Cordier, J.-Y. Mevellec, F. Massuyeau, C. Latouche, C. Martineau-Corcos and S. Perruchas, *Inorg. Chem.*, 2020, **59**, 13607–13620.
18 D. Bissessar, J. Egly, T. Achard, P. Steffanut, M. Mauro and S. Bellemin-Laponnaz, *Eur. J. Inorg. Chem.*, 2022, e202200101.
19 R. Utrera-Melero, M. Cordier, F. Massuyeau, J.-Y. Mevellec, A. Rakhmatullin, C. Martineau-Corcos, C. Latouche and S. Perruchas, *Inorg. Chem.*, 2023, **62**, 18157–18171.
20 A. K. Gupta and A. Orthaber, *Chem. – Eur. J.*, 2018, **24**, 7536–7559.
21 K. Škoch, I. Císařová and P. Štěpnička, *Inorg. Chem.*, 2014, **53**, 568–577.
22 V. W.-W. Yam, C.-H. Lam and N. Zhu, *Inorg. Chim. Acta*, 2002, **331**, 239–245.
23 K. Brantin, M. Håkansson and S. Jagner, *J. Organomet. Chem.*, 1994, **474**, 229–236.
24 M. Håkansson, K. Brantin and S. Jagner, *J. Organomet. Chem.*, 2000, **602**, 5–14.
25 B. M. Mykhalichko, M. G. Mys'kiv and E. A. Goreshnik, *Russ. J. Coord. Chem.*, 1999, **25**, 65–69.
26 T. Jiang, K. Zhang, Y. Shen, M. Hamdaoui, R. Dontha, J. Liu, B. Spingler and S. Duttwyler, *Dalton Trans.*, 2019, **48**, 17192–17199.
27 C. Martín, M. Sierra, E. Alvarez, T. R. Belderrain and P. J. Pérez, *Dalton Trans.*, 2012, **41**, 5319–5325.
28 N. Nagapradeep, V. Venkatesh, S. K. Tripathi and S. Verma, *Dalton Trans.*, 2014, **43**, 1744–1752.
29 U. Létinois-Halbes, P. Pale and S. Berger, *J. Org. Chem.*, 2005, **70**, 9185–9190.
30 J. C. Dyason, P. C. Healy, L. M. Engelhardt, C. Pakawatchai, V. A. Patrick, C. L. Raston and A. H. White, *J. Chem. Soc., Dalton Trans.*, 1985, **4**, 831–838.
31 A. Gallego, C. Hermosa, O. Castillo, I. Berlanga, C. J. Gómez-García, E. Mateo-Martí, J. I. Martínez, F. Flores, C. Gómez-Navarro, J. Gómez-Herrero, S. Delgado and F. Zamora, *Adv. Mater.*, 2013, **25**, 2141–2146.
32 S. Lal, J. McNally, A. J. P. White and S. Díez-González, *Organometallics*, 2011, **30**, 6225–6232.
33 The CCH angles are also distorted from linearity (all angles approx. 143°), but due to the uncertainty of the H position these angles are not discussed further.
34 E. Weisheim, C. G. Reuter, P. Heinrichs, Y. V. Vishnevskiy, A. Mix, B. Neumann, H.-G. Stammler and N. W. Mitzel, *Chem. – Eur. J.*, 2015, **21**, 12436–12448.
35 J. L. Kiplinger, A. M. Arif and T. G. Richmond, *Organometallics*, 1997, **16**, 246–254.
36 A. F. Hill, N. Tshabang and A. C. Willis, *Eur. J. Inorg. Chem.*, 2007, 3781–3785.
37 H. Yasuda, H. Yamamoto, T. Arai, A. Nakamura, J. Chen, Y. Kai and N. Kasai, *Organometallics*, 1991, **10**, 4058–4066.
38 A. Noonikara-Poyil, S. G. Ridlen, I. Fernández and H. V. R. Dias, *Chem. Sci.*, 2022, **13**, 7190–7203.
39 This Cu atom shows a positional disorder Cu7A (0.093) and Cu7 (0.907).
40 L.-M. Zhang and T. C. W. Mak, *J. Am. Chem. Soc.*, 2016, **138**, 2909–2912.
41 L. L.-M. Zhang and T. C. W. Mak, *Angew. Chem., Int. Ed.*, 2017, **56**, 16228–16232.
42 M.-M. Zhang, X.-Y. Dong, Z.-Y. Wang, H.-Y. Li, S.-J. Li, X. Zhao and S.-Q. Zang, *Angew. Chem., Int. Ed.*, 2020, **59**, 10052–10058.
43 (*a*) CCDC 2239140: Experimental Crystal Structure Determination, 2025, DOI: **10.5517/ccdc.csd.cc2f50bz**; (*b*) CCDC 2239141: Experimental Crystal Structure Determination, 2025, DOI: **10.5517/ccdc.csd.cc2f50c0**.

